The vapour-screen method of flow visualization

By I. McGREGOR
Royal Aircraft Establishment, Bedford

(Received 1 April 1961)

The vapour-screen method of flow visualization in supersonic wind tunnels is outlined, and the development of a suitable technique for use in the 3 ft. tunnel at R.A.E. Bedford described, together with the associated optical and photographic equipment.

The results of tests to determine the humidity required to produce an optimum density of fog in the working section over the Mach number range 1·3–2·0 are presented and the influence of tunnel pressure and temperature discussed. Numerous vapour-screen photographs of the flow over and behind delta wings are included and some comparisons made with the corresponding surface oil-flow patterns.

The process of condensation, the physical and optical properties of the resulting fog, and the formation of the vapour-screen picture are all considered in some detail.

The effects of humidity on the Mach number and static pressure in the working section were investigated and the results are compared with theoretical estimates at a nominal Mach number of 2·0. It is shown that the adverse effects of condensation on the flow at high Mach numbers may be alleviated by the use of liquids with a lower latent heat of evaporation than water, and some results obtained at a Mach number of 2·0 using carbon tetrachloride vapour are described.

The possibility of extending the vapour-screen technique to transonic and subsonic speeds is also considered, and some results obtained at a Mach number of 0·85 are included.

1. Introduction

The vapour-screen method of flow visualization in supersonic wind tunnels was first employed by Allen & Perkins (1951), and since then has been used occasionally in other experimental investigations, such as those of Gapcynski (1955), Hall, Rogers & Davies (1957), and Jorgensen (1957). The principle of the method is very simple. The tunnel is run with moist air, and as the air expands through the supersonic nozzle into the working section it cools, and the moisture condenses out to form a fog. This is then illuminated by a narrow beam of light perpendicular to the axis of the tunnel. Any disturbance in the cross-flow plane, such as that caused by a model at incidence, disturbs the uniform distribution of fog particles in the plane of the vapour screen, and hence the amount of light scattered by the fog. In particular, wakes and vortices from wings and bodies

appear as dark 'holes' in the screen. However, very little information is available concerning such aspects of technique as the humidity required to produce a satisfactory screen at different Mach numbers and how this is influenced by such factors as tunnel pressure and temperature, or of the effects of the condensing vapour on the flow in the working section.

An extensive research programme on types of flow at transonic and supersonic speeds over wings of various planforms, thickness-chord ratios and section shapes is in progress in the 3 ft. tunnel at R.A.E. Bedford, and it was felt that the vapour-screen method could usefully supplement results obtained from force measurements and surface oil-flow patterns. In particular, information was sought concerning the size and shape of any vortices or regions of separated flow existing over the surfaces of the wings. It was considered that, to fulfil this function adequately, it would be necessary to achieve a rather better resolution of detail than appears to have been realized up to now. The present investigation was therefore undertaken to examine the suitability of the method for this purpose, to develop a suitable experimental technique, and to establish optimum operating conditions over a range of Mach number.

2. Experimental equipment

2.1. *The 3 ft. wind tunnel*

The wind tunnel used for these tests is continuous running, with a working section 3 ft. square, and supersonic Mach numbers between 1·3 and 2·0 are generated by a series of interchangeable blocks that form a single-sided nozzle upstream of the working section. The tunnel is driven by two centrifugal compressors in series. The total pressure can be varied between 3 in. and 60 in. of mercury by means of a compressor-evacuator set. Cooling arrangements consist of (*a*) an intercooler between the two compressor stages, and (*b*) an aftercooler, with a rather greater capacity than the intercooler, situated in the maximum section of the tunnel immediately before the contraction. The flow of water through the intercooler is continuously variable, but only coarse control of the aftercooler is possible. Drying of the air in the tunnel is effected by by-passing a fraction of the air through driers charged with silica gel which are connected across the second stage of the compressor. The quantity of air passing through the driers is controlled by a motorized flap valve, and with the driers in reasonably good condition a humidity corresponding to a frost-point of about -40 °C is obtained after 10–15 min. running. The total volume of the tunnel is approximately 45,000 ft.^{3}, and this humidity represents about 0·3 lb. of water vapour remaining in the tunnel circuit.

2.2. *Optical system*

It was considered that the illumination system should provide a beam of light that was (*a*) as intense as possible, (*b*) narrow, with little variation in width across the working section, and (*c*) sharp-edged, so that a minimum of stray light entered the tunnel.

The light source selected was a 1000 W high-pressure mercury-vapour lamp with an effective length of 7·5 in. and an external diameter of approximately

0·5 in. The problem was to produce a beam of light that would satisfy the above requirements. The simplest arrangement—a slit with the lamp behind it—was rejected on the grounds that to produce a suitable beam would have entailed placing the lamp at least 2 ft. behind the slit, and this would cause an excessive loss of illumination. A system using cylindrical lenses was next examined, but it was considered that the intensity of illumination would not be materially better than that given by a simple slit when the beam was satisfactory in other respects.

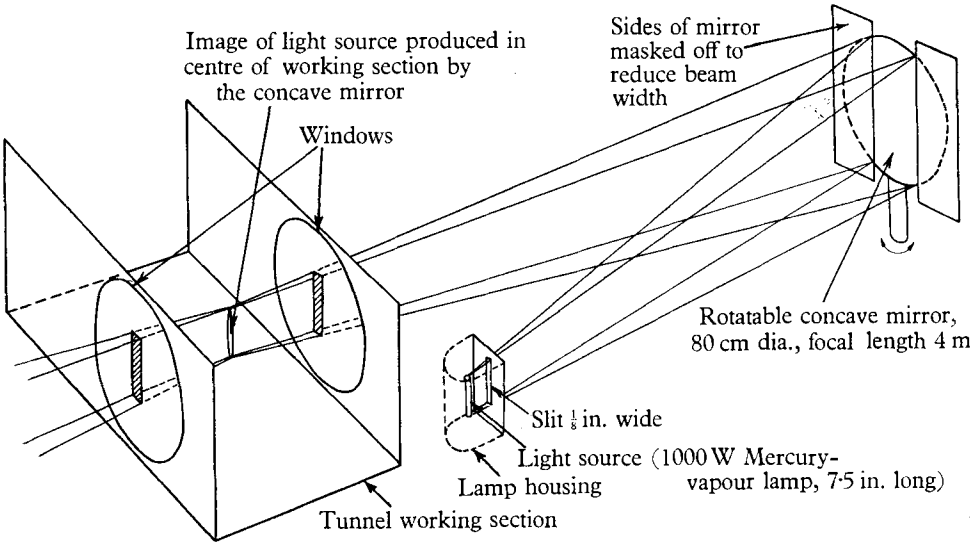

FIGURE 1. Illumination system for vapour-screen experiments.

The arrangement finally adopted made use of one of the mirrors from the tunnel Schlieren system, and proved to be very effective. It is shown in figure 1. The 80 cm diameter concave mirror with a focal length of 4 m was used to produce an image of the light source in the centre of the working section. To reduce the width and lateral spread of the beam, a slit 0·1 in. wide was placed just in front of the lamp and the sides of the mirror masked, leaving an effective area of mirror 32×10 in. This arrangement produced a sharp-edged beam of light approximately 0·15 in. wide by 9 in. high in the centre of the working section. Both the height and width of the beam increased slightly away from the centre line, but even at the windows the width of the beam was only about 0·5 in.

It was not feasible to move the mirror backwards and forwards to track the beam of light along the working section, and this was accomplished by rotating the mirror about its vertical axis. As a result, the beam was perpendicular to the centre line of the tunnel in only one position, but the maximum deviation of the beam from the perpendicular did not exceed 2°.

2.3. *Photographic equipment*

The easiest way to photograph the vapour screen is from the side of the tunnel. However, whilst this is adequate for some purposes, the screen is inevitably viewed at an appreciable angle, and it is difficult to locate the position of any

vortices that may be present relative to the model. It was therefore decided to photograph the screen from directly downstream. A remotely controlled camera was used, mounted at the root of the model sting support. The camera, which was driven by clockwork, gave negatives approximately 1 in. square on standard 35 mm film. The shutter was operated by a solenoid mounted alongside the camera, but it was not possible to alter the focus from outside the tunnel.

The wing of a model remote from the light source is in a shadow cast by the sting or body, so that in general it is necessary for the field of view of the camera to contain only the body and the wing panel nearer the light source. The camera was therefore fitted with a telephoto lens of 7·5 cm focal length, which gave a field of view approximately 10 in. square at a position corresponding to the trailing edge of a typical 3 ft. tunnel model, and the camera was mounted at a small angle to the centre-line of the sting to enable the wing tip of the largest model to be included in the picture.

The camera and its operating solenoid were housed in a cowl constructed from brass sheet, with a plate glass window 0·25 in. thick to protect the lens. However, this cowling caused considerable blockage and it proved impossible to start the tunnel at $M = 1{\cdot}3$, but no trouble was experienced at higher Mach numbers.

3. Experimental technique

3.1. *Humidity control*

It is necessary to be able to exercise careful control of the humidity if optimum results are to be obtained. The procedure evolved for the present tests consisted of running the tunnel at the desired total pressure with the driers in circuit for a period of about 15 min. The driers were then switched out, and a measured quantity of water injected into the tunnel. In all the work so far undertaken the tunnel has been run at a total pressure below atmospheric, and the water was simply sucked in through a static-pressure tapping in the wall of the diffuser, where vaporization was almost instantaneous.

3.2. *Temperature control; effect of the aftercooler*

For the first few tests the tunnel was run in the normal manner with both the intercooler and aftercooler in operation. However, it was found that the fog produced in the working section was extremely patchy and irregular, some parts being practically devoid of any condensation, while in others there were streamers of thick fog. This suggested that the temperature distribution across the working section was uneven, so a total-temperature probe was constructed to measure the distribution. The probe consisted of a tube mounted across the centre of the working section with a number of thermocouples arranged along its leading edge. The result of a typical survey is given in figure 2, which shows a temperature difference of some 20 °C between the 'hotspot' near the centre of the tunnel and the colder air at the sides. Overhaul of the aftercooler effected some improvement in the temperature distribution, but only a slight improvement in the distribution of fog resulted, and it was still considered to be far too uneven to be acceptable.

The effect of switching off the aftercooler was then examined. This meant that, apart from heat losses from the tunnel shell, the intercooler alone was responsible for cooling, which limited the power input if overheating was to be avoided. As a result the tunnel could only be run at a considerably reduced total pressure. The overheating problem was most serious at the top end of the Mach number range, when the mass flow of air around the tunnel circuit was low, but the pressure ratio across the compressors high. However, it was found that this arrangement gave a perfectly uniform fog in the working section, although it was

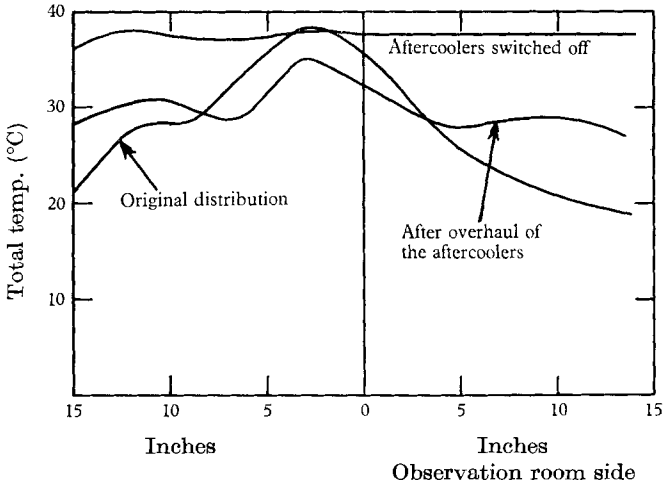

FIGURE 2. Temperature distribution across the working section of the tunnel.

first necessary to wait until the tunnel total temperature attained a reasonably steady value. For the first run of the day this warming-up period was of the order of an hour, but for subsequent runs 10–15 min sufficed. The only disadvantage was that, as the intercooler was always operating at or very near maximum capacity, it was not possible to investigate the effect of total temperature on fog formation.

3.3. *Photographic details—determination of the 'optimum fog density'*

From the photographic point of view, the optimum fog density is a compromise between two conflicting requirements. If the fog is too thin, a long exposure time is needed and there is a risk of light reflexion from the model and the walls of the tunnel obscuring the low-contrast vapour-screen picture. On the other hand, if the fog is too thick, there is excessive scattering of light by the fog between the plane of the vapour screen and the camera lens which results in a very 'grainy' picture with blurred detail.

A series of tests was therefore carried out with fogs of different densities, photographing the vapour-screen picture produced by a model at incidence, over a range of exposure times from 5 to 80 sec. The camera was set at an aperture of $f/4$ and FP 3 film used. Best results were obtained with what appeared to be a quite thin fog as viewed from the side of the tunnel. The corresponding exposure time was 20 sec.

Light reflexion from the model was reduced by painting it with camera black and stray light entering the working section was kept to a minimum by masking the side windows, leaving only a slit wide enough for the main light beam to enter.

The combination of long focal-length lens (7·5 cm) and wide aperture setting ($f/4$) resulted in a depth of focus of only $\pm 0{\cdot}8$ in. at the range normally used (3–4 ft.). However, it proved possible to take photographs with no detectable loss of clarity 2 in. from the nominal focal point, so the screen could be photographed at axial positions up to 4 in. apart without the need for refocusing.

4. Experimental results and discussion

4.1. *Scope of tests*

Tests were made to determine the quantity of water required to produce a photographically-suitable vapour-screen at Mach numbers between 1·3 and 2·0. The effects of humidity on the flow in the working section were also investigated and measurements made of the static pressure and Mach number.

4.2. *Presentation of humidity results*

The accepted practice is to present experimental results for tunnel humidity in a non-dimensional form, but in this case care is necessary if the results are not to be misleading. For example, although tunnel total pressure was found to have some effect, the degree of condensation, and therefore of fog density, depends essentially on the amount of water present in the tunnel and not on the water/air ratio. It is therefore not relevant to express the humidity in terms of lbs of water/lb. of air ('absolute humidity'), as is normally done when condensation effects in wind tunnels are being discussed and the amount of heat given up to the air by the vapour as it condenses is of prime importance. The stagnation relative humidity (the ratio of the actual vapour density to the density of saturated vapour at the same temperature) is independent of stagnation pressure, but is a function of stagnation temperature, so this is also unsuitable. A parameter which avoids these defects is the frost-point, which defines a unique relation between the quantity of water vapour and the volume of the tunnel which is independent of stagnation conditions. A curve showing the frost-point as a function of the quantity of water added to the nominally 'dry' tunnel is presented in figure 3, a mean frost-point for the 'dry' tunnel of -41 °C having been assumed. A few experimental measurements are included and these show quite good agreement with the theoretical curve. However, the quantity of water–frost-point relationship is logarithmic in character and whilst very sensitive at low humidities, in the range of interest of these tests the sensitivity is only of the order of 2 °C change in frost-point per pint of water added. In view of this fact, and of the difficulty of making reliable frost-point measurements, it was decided that the most straightforward way to describe the humidity was directly in terms of quantity of water added to the 'dry' tunnel, but scales showing the frost-point or absolute humidity (when the effects of condensation on static pressure and Mach number are being considered) have been added to the figures where appropriate.

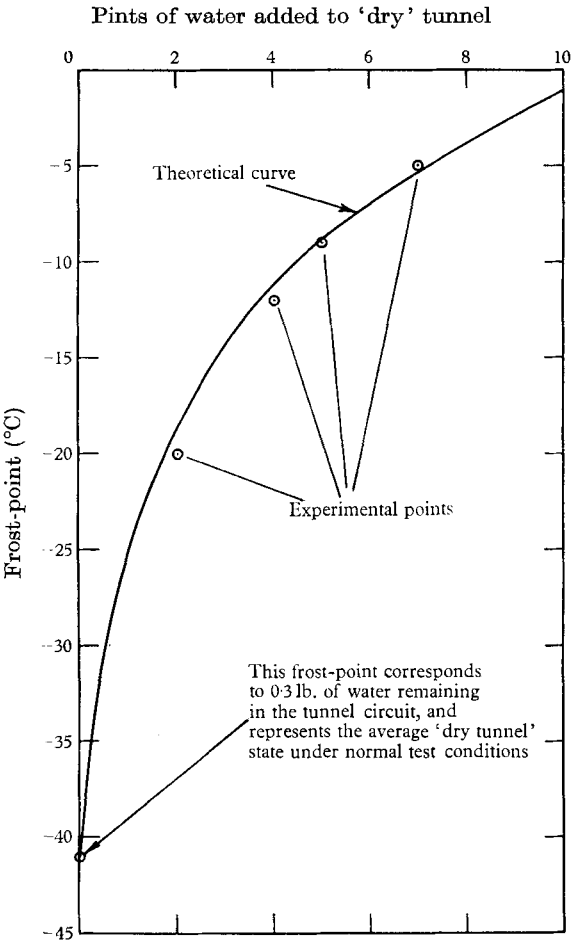

FIGURE 3. Relation between the quantity of water added to the tunnel and the frost-point.

4.3. *Quantity of water required to produce a satisfactory vapour screen*

As described in § 3.3, the optimum fog density was found by injecting measured quantities of water into the tunnel and photographing the resulting vapour screen. Examination of the photographs then gave an optimum range of humidity. This detailed determination was only carried out at two Mach numbers, 1·51 and 1·81, and for other Mach numbers the range of humidity over which a satisfactory screen was produced was estimated visually. The results of these tests are presented in figure 4. The results for the various Mach numbers were not obtained at exactly the same total pressure and temperature, but are substantially correct for a value of $p_t = 12$ in. of mercury and $T_t = 45$ °C. It must be mentioned here that the Mach number quoted is that developed by the nozzle with dry air: above about $M = 1{\cdot}6$ there is a marked humidity effect on the flow and the actual Mach number when a vapour screen is present is considerably less than with dry air.

Several points of interest arise from this curve. The limits of the humidity range for a satisfactory vapour screen are a subjective matter not capable of precise determination, but, even allowing for this, the range of humidity over which a satisfactory screen is produced is quite small; the humidity at which the fog density tends to be too thick is only some 25–30 % greater than that at which it tends to be too thin. Secondly, there is the very rapid increase in humidity required at Mach numbers less than 1·5. The quantity of water vapour

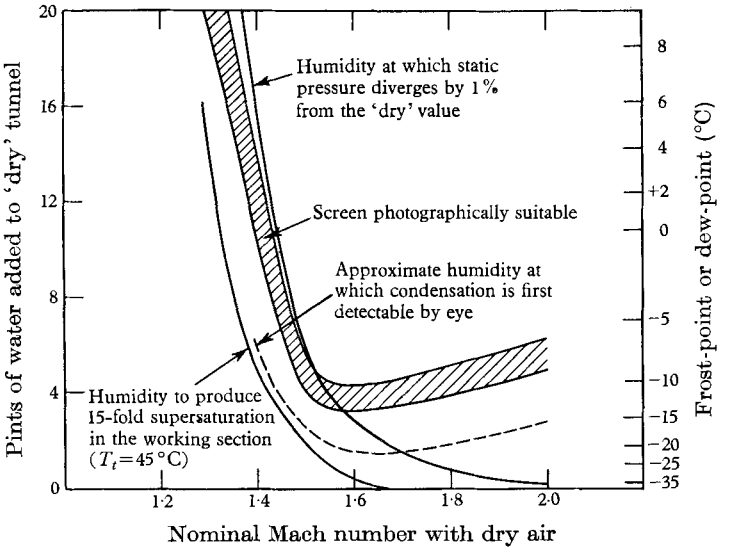

FIGURE 4. Effect of Mach number on the quantity of water required to produce a satisfactory vapour screen. Total pressure = 12 in. Hg, total temperature = 45 °C.

required to saturate a given volume increases very rapidly with temperature at low temperatures (figure 5), and the higher working section static temperature at the lower Mach numbers is sufficient to cause a large increase in the humidity necessary for saturated flow in the working section. It is well known that a considerable degree of supersaturation is necessary to cause condensation in a supersonic nozzle, so a curve has been added to figure 4, which shows the quantity of water required to produce a 15-fold supersaturation in the working section at a total temperature of 45 °C, the assumption being made that the working section static temperature is the same as with dry air. It is seen that this curve is very similar in shape to that denoting the quantity of water required to produce a satisfactory vapour screen. The third feature is that the humidity required reaches a minimum value at a Mach number of about 1·6 and thereafter shows a slight increase. Above M = 1·6, it seems likely that virtually all the water added to the tunnel is condensed out, so that if the fog is to be of constant density then the stagnation humidity must increase to allow for the greater expansion of the flow with increasing Mach number, i.e. the quantity of water it is necessary to add will vary inversely with the density in the working section.

There are no theoretical reasons for supposing that the quantity of water required to produce a satisfactory vapour screen can be simply expressed in

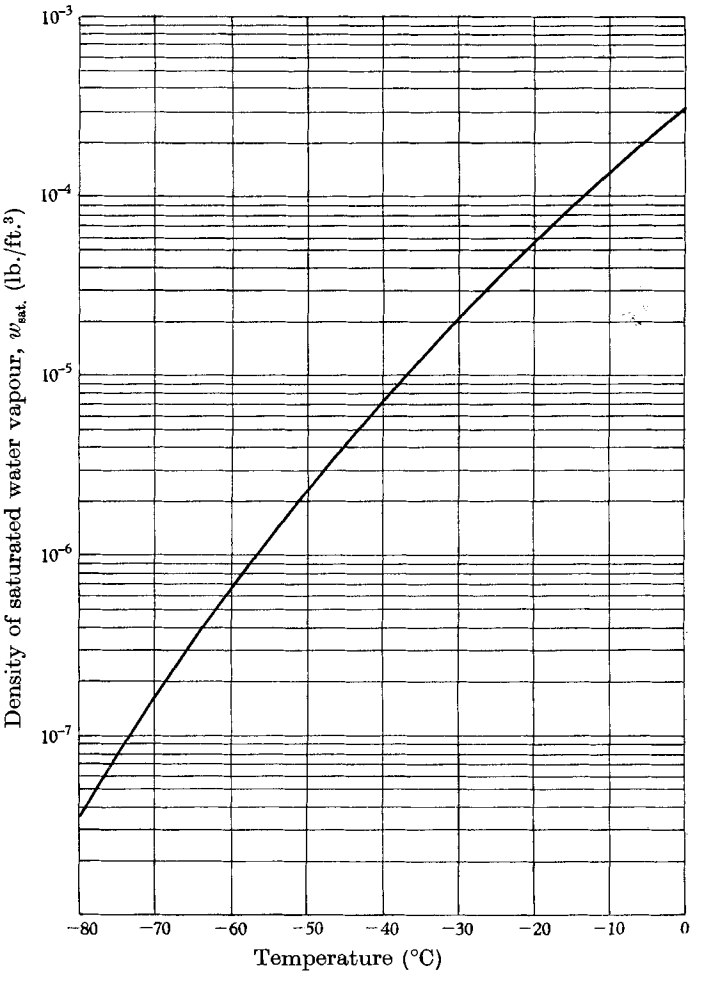

FIGURE 5. Density of saturated water vapour as a function of temperature.

terms of known properties of the flow, but as a reasonable approximation over the experimental range it is given by

$$\left(\frac{\rho}{\rho_t}\right)\frac{W}{V} = 18w_{\text{sat.}} + 0{\cdot}00003,$$

where W = quantity of water required to produce a satisfactory vapour screen (lb.),

V = total volume of the tunnel (45,000 ft.^{3}),

ρ_t = stagnation density of the air,

ρ = density of air in the working section (assuming isentropic flow),

$w_{\text{sat.}}$ = density of saturated water vapour at the working section static temperature under isentropic conditions (lb./ft.^{3}).

The variation of $w_{\text{sat.}}$ with temperature is shown in figure 5. The volume of the working section is small compared with that of the settling chamber so that $(\rho/\rho_t)\,W/V$ is approximately equal to the density of the mixture of fog and un-

condensed water vapour in the working section. The factor 18 may be considered as the degree of supersaturation necessary to cause condensation and 0·00003 lb./ft.^{3} as the mean density of the condensed fog particles in the working section, but this interpretation should not be taken too literally.

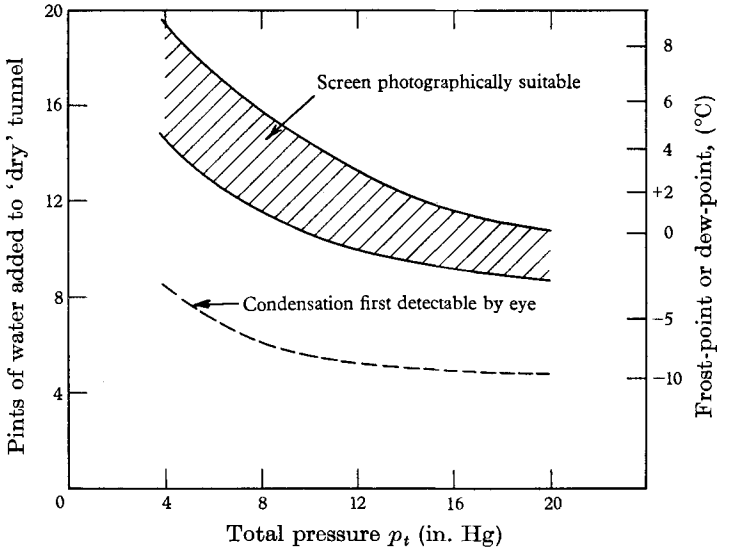

FIGURE 6. Effect of tunnel total pressure on the quantity of water required to produce a satisfactory vapour screen at a Mach number of 1·41. Total temperature = 44 °C.

It was mentioned earlier that it was not possible to investigate the effects of total temperature on fog formation, but some idea of its effect on the quantity of water required may be gained from the above equation. The critical parameter is the working section static temperature, T_s. When this is less than about -60 °C, the term $18w_{\text{sat.}}$ is negligible in comparison with 0·00003, so that provided T_s continues to be less than about -60 °C, changing T_t will have little effect. However, if a change in T_t causes T_s to rise appreciably above -60 °C, the magnitude of the term $18w_{\text{sat.}}$ increases very rapidly and so the humidity will have to be increased to maintain a satisfactory vapour screen.

The effects of tunnel total pressure on fog formation were investigated at a nominal Mach number of 1·41. The total pressure p_t was varied between 18 and 4·5 in. of mercury, and T_t held at 44 °C ($\pm 0{\cdot}5$ °C). The results are presented in figure 6 and show that as the total pressure was reduced, an increasing quantity of water had to be added to the tunnel to produce a satisfactory vapour screen. A possible explanation for this is as follows. When the water vapour condenses to form droplets of liquid water, the latent heat of evaporation is liberated and absorbed by the surrounding air, causing a rise in temperature. If the total pressure is reduced, the amount of heat absorbed by the air per unit mass of water vapour condensed is unchanged, but since there is a smaller mass of air the rise in temperature is greater. This rise in working section static temperature increases the saturated vapour density in the working section, so a greater initial humidity is necessary to produce the same amount of condensation.

At Mach numbers above about 1·6 it is expected that the effect of total pressure will not be so marked as at $M = 1{\cdot}41$, since then a much greater proportion of the water vapour present is condensed out in the working section.

4.4. *Physical appearance and characteristics of the vapour screen*

On the addition of a small quantity of water to the 'dry' tunnel no visible condensation could be detected, even if, as occurred at nominal Mach numbers of 1·81 and 2·00, a rise in working section static pressure indicated that a condensation shock was present. On further increasing the humidity, a point was reached where the outline of the beam of light could just be discerned in the working section, giving rise to a very faint, deep blue vapour screen. The approximate humidity at which this blue haze could first be detected was noted and is plotted as a function of Mach number in figure 4 and of total pressure in figure 6. In both cases it is seen to vary in a similar manner to the quantity of water required to produce a satisfactory vapour screen.

Further development of the vapour screen with humidity depended on Mach number. At Mach numbers up to and including 1·51, the screen at first became slightly denser, but it then gradually acquired an iridescent character in which wide vertical bands of violet, blue, green and yellowish green light could be clearly seen when viewed from a suitable position. At the higher Mach numbers, the blue haze just became denser and slightly paler in colour.

The optical properties of fogs are rather complex and it is not proposed to enter into a detailed study here, but some consideration of the observed phenomena can yield interesting information concerning certain physical characteristics of the fog. Suppose a beam of light is projected through air containing a large number of very small particles in suspension (of radius less than 10^{-5} in., say), whose size is small relative even to the wavelength of visible light (wavelength $1{\cdot}6 \times 10^{-5}$ to $2{\cdot}7 \times 10^{-5}$ in.). In such circumstances a scattering of the light will take place (Tyndall effect), the scattering being much more pronounced for light of the shorter wavelengths than for the long. It is believed that such light scattering was responsible for the bluish colour of the vapour screen when the humidity was such that condensation could first be detected by eye. On increasing the humidity, the fog particles increase in size. True scattering will also increase (in proportion to the increase in surface area of the particles) and will tend to occur more equally for light of all wavelengths, but effects due to diffraction of the light may also become important if the particles exceed a certain critical size. With a spherical particle, the intensity of the diffracted light passes through a series of maxima and minima in directions making an angle θ with the original direction of the beam, given by the classical diffraction formula $\sin\theta = k\lambda/r$, where λ = wavelength of the light, r = radius of the spherical particle and k = a constant. The first maximum occurs when $k = 0$ (undeflected light), and the first minimum when $k = 0{\cdot}61$. Further maxima occur when $k = 0{\cdot}810$ and 1·333, and minima when $k = 1{\cdot}116$ and 1·619. The intensity with $k = 0{\cdot}810$ is only 1·7 % of the incident light and the subsequent intensity maxima are smaller still. However, it follows that for each wavelength there are certain

directions relative to the direction of the incident light along which light of that particular wavelength has a maximum or minimum intensity, so the diffracted light is split up into a spectrum. In the case of the vapour screen, there is a very large number of illuminated water droplets, each diffracting some of the light striking them, so that viewed at an angle from the side of the tunnel, bands of coloured light might be expected to appear across the screen in spectral order, with red nearest the observer (long wavelength and correspondingly large value of θ for maximum intensity). This is in agreement with observation at Mach numbers between 1·3 and 1·5, with the exception that no red or orange bands were detected. A possible explanation for the absence of these colours is discussed later.

The existence of these coloured bands implies that all (or the greater part) of the water droplets forming the fog must be of nearly uniform size. If there is a variation in size, each droplet will diffract the light differently. With a large number of droplets whose size varies in a random manner, the resultant diffracted light would presumably appear white, since if a particular direction were the direction for maximum intensity for a certain wavelength from one droplet, there would be other droplets for which this direction was the direction of maximum intensity for other wavelengths, giving, in effect, a continuous spectrum.

It is possible to obtain an estimate of the size of the droplets in the fog by observation of the coloured bands in the vapour screen. A test was made at a Mach number of 1·41, with a total presure of 12 in. Hg and a total temperature of 46 °C. With 11 pints of water added to the 'dry' tunnel (the quantity necessary to produce a satisfactory vapour screen under these conditions), it was found that the first and second intensity maxima for blue light occurred at angles of 30° and 55° respectively to the direction of the original light beam. The wavelength of blue light is approximately $1{\cdot}8 \times 10^{-5}$ in., so from the first maximum we have

$$r_1 = \frac{0{\cdot}810 \times 1{\cdot}8 \times 10^{-5}}{\sin 30^\circ} = 2{\cdot}9 \times 10^{-5} \text{ in.},$$

and from the second

$$r_2 = \frac{1{\cdot}333 \times 1{\cdot}8 \times 10^{-5}}{\sin 55^\circ} = 2{\cdot}9 \times 10^{-5} \text{ in.}$$

Such perfect agreement between the two results must be considered fortuitous, since it was not possible to measure the angles to better than about 2°, but it may be concluded fairly confidently that in this case the radius of the droplets is about 3×10^{-5} in. This is of the same order as the size of the droplets in an artificial fog (produced by the sudden expansion of some wet air in a flask) as measured by Stodola (1927), using a light-diffraction method.

It was mentioned above that no red or orange bands were observed in the vapour screen. Assuming a droplet radius of $2{\cdot}9 \times 10^{-5}$ in., the first maximum for red light should occur at an angle

$$\theta = \sin^{-1}\left(\frac{0{\cdot}810 \times 2{\cdot}7 \times 10^{-5}}{2{\cdot}9 \times 10^{-5}}\right) = 49^\circ.$$

The second maximum for violet light will occur at an angle

$$\theta = \sin^{-1}\left(\frac{1{\cdot}333 \times 1{\cdot}6 \times 10^{-5}}{2{\cdot}9 \times 10^{-5}}\right) = 47°.$$

There is thus some overlapping of the first maximum for light of long wavelength with the second maximum for light of short wavelength. Now the spectrum of the mercury vapour lamp is rich in blue and violet light but rather deficient in red and orange, so that although the second maximum for violet is less intense than the first, it is probably still stronger than the first maximum for red or orange. This offers a plausible reason why the red or orange bands could not be detected.

With regard to the change in character of the screen between Mach numbers of 1·5 and 1·6, it seems probable that this is due to a change in the mechanism of condensation, which results in a greater number of smaller particles being formed at the higher Mach numbers, so that dispersion of light by the fog remains a true scattering effect without diffraction. In addition to this change in size, a change in the nature of the fog particles from water droplets to ice crystals is also likely, although the two effects are not related. It is known from the work of Mason (1957) and others that small droplets of pure water can be supercooled to approximately $-40\,°C$ before freezing takes place, when cooled slowly. With droplets formed during the rapid expansion of saturated water vapour, an even greater degree of supercooling appears necessary, and Sander & Damköhler (1953) have shown that under such conditions, a temperature of approximately $-62\,°C$ is required before ice crystals form. It may be that at these low temperatures the vapour condenses directly into ice crystals without passing through the liquid phase, but this point is uncertain. However, a temperature of $-62\,°C$ corresponds to the working section static temperature at a Mach number of 1·59 under isentropic conditions and with a total temperature of 45 °C, so that at the higher Mach numbers the observed fog almost certainly consisted of ice crystals.

4.5. *The mechanism of condensation*

A saturated or supersaturated vapour will condense only if there are 'condensation nuclei' present. These nuclei can be of two forms—minute particles of dust or other foreign matter, and nuclei which are generated spontaneously in the vapour by random molecular aggregation. Nuclei of the former type are invariably present to a greater or lesser degree, but whilst groups of molecules are continually forming in any gas or vapour, they are unstable and immediately break up again, and so cannot form condensation nuclei unless the vapour is heavily supersaturated. When condensation occurs on foreign nuclei, the number of droplets formed per unit volume is limited by the number of nuclei present, and the rate at which the vapour condenses is determined by the rate at which the droplets can grow, which in turn depends on the degree of supersaturation, the rate of diffusion of vapour molecules on to the surface of the droplets and the rate of transfer of the latent heat of evaporation away from the droplets. On the other hand, with self-generated nuclei, the number of nuclei per unit volume can reach astronomical figures when the vapour is sufficiently

supersaturated and condensation can take place extremely rapidly (condensation 'shock'), leading to a very large number of minute droplets. These two condensation processes and their relative importance in wind tunnels were first discussed in detail by Oswatitsch (1941), who concluded that in supersonic tunnels the effects of foreign nuclei could be neglected. In the present case, however, it is believed that at Mach numbers up to and including 1·51, condensation is occurring principally on foreign nuclei and that only at higher speeds do self-generated nuclei become predominant. The reasons leading to the adoption of this conclusion are discussed at some length in Appendix I. It must be emphasized that this conclusion is only valid for the 3 ft. tunnel for the particular conditions under which it was operated, and does not necessarily apply in general. It is shown, for instance, that a reduction in total temperature considerably decreases the importance of foreign condensation nuclei. The question of tunnel size is also considered briefly and it is concluded that in a smaller tunnel a greater stagnation humidity will be necessary to produce the same density of fog in the working section at the same total pressure and Mach number.

4.6. *Effect of humidity on working-section static pressure and Mach number*

Measurements were made of the variation of the working section static pressure with the quantity of water added to the tunnel at several Mach numbers, and the results, expressed as the ratio of the actual static pressure to the pressure with dry air, p/p_{dry}, are presented for nominal Mach numbers of 1·51, 1·81 and 2·00 in figures 7 and 8. The actual Mach number in the working section was measured at nominal Mach numbers of 1·51 and 2·00 by sticking strips of cellulose tape approximately 0·003 in. thick on the top and bottom walls of the tunnel just ahead of the windows. These generated very weak shock waves (effectively Mach waves), which were photographed using the tunnel Schlieren system. The included angle between the two waves (equal to twice the Mach angle) was measured from photographic enlargements and the actual Mach number obtained. The variation of actual Mach number with humidity is shown in figure 8.

At Mach numbers less than 1·51, it is possible to obtain sufficient condensation to produce a satisfactory vapour screen without affecting either the working section static pressure or Mach number. In this Mach number range it is believed that condensation is occurring progressively on foreign condensation nuclei without a condensation shock. At the higher Mach numbers a condensation shock is clearly present, and at a certain humidity the static pressure suddenly starts to increase and the working section Mach number to decrease. The humidity at which the static pressure diverges by 1 % from the 'dry' value is a convenient indication of the onset of the condensation shock, and this humidity is shown as a function of Mach number in figure 4 for a stagnation pressure of 12 in. Hg.

It will be noted from figure 4 that at $M = 1{\cdot}81$ and 2·00 a condensation shock occurs at a lower humidity than that at which fog is first visible in the working section, whilst at Mach numbers less than 1·6 there may be visible condensation without a condensation shock. Thus, as has been previously pointed out by Oswatitsch (1941), the appearance or disappearance of fog in the working section is not a reliable guide to the presence or absence of condensation effects.

Once a condensation shock is established, the working section static pressure does not necessarily increase steadily with increasing humidity. At both $M = 1{\cdot}81$ and 2·00 (figures 7 and 8) there is a range of humidity, soon after the condensation

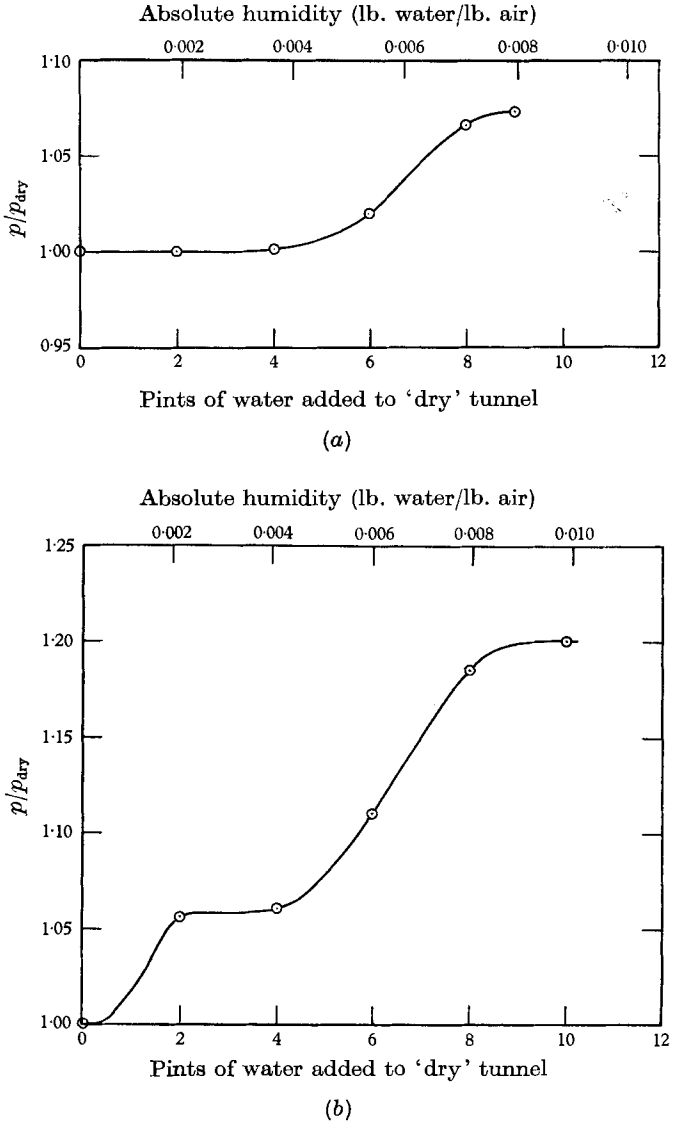

FIGURE 7. Effect of humidity on working-section static pressure at nominal Mach numbers of 1·51 and 1·81. (*a*) $M_{dry} = 1{\cdot}51$; total pressure = 13·2 in. Hg; total temperature = 44 °C. (*b*) $M_{dry} = 1{\cdot}81$; total pressure = 12·0 in. Hg; total temperature = 48 °C.

shock forms, over which the static pressure is constant, and at $M = 1{\cdot}51$ and 1·81, at the maximum humidity investigated, the rate of increase of pressure with humidity is again nearly zero. The reason for this is uncertain, but it may be associated with the passage of a reflexion of the condensation shock across the tunnel static-pressure tappings. At a nominal Mach number of 2·0, the actual

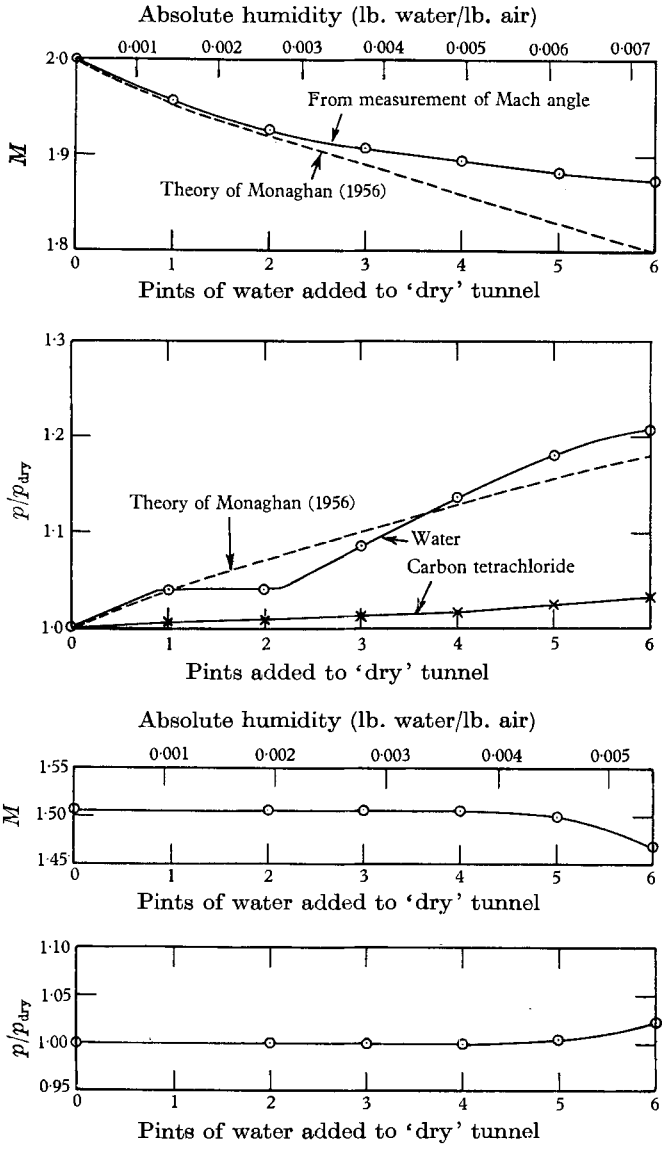

FIGURE 8. Effect of humidity on actual Mach number and static pressure in the working section at nominal Mach numbers of 2·00 and 1·51. (*a*) $M_{dry} = 2{\cdot}00$; total pressure = 9·0 in. Hg; total temperature $\simeq 47\,^{\circ}\mathrm{C}$. (*b*) $M_{dry} = 1{\cdot}51$; total pressure = 13·2 in. Hg; total temperature = 42 °C.

Mach number in the centre of the working section decreases monotonically with increasing humidity and does not show any discontinuities. The rate of decrease of Mach number with humidity is greatest immediately after the condensation shock forms.

Making the assumption that the flow is one-dimensional and isentropic before and after condensation shock, Monaghan (1956) has derived certain approximate relations (see Appendix II) for the working section static pressure and Mach

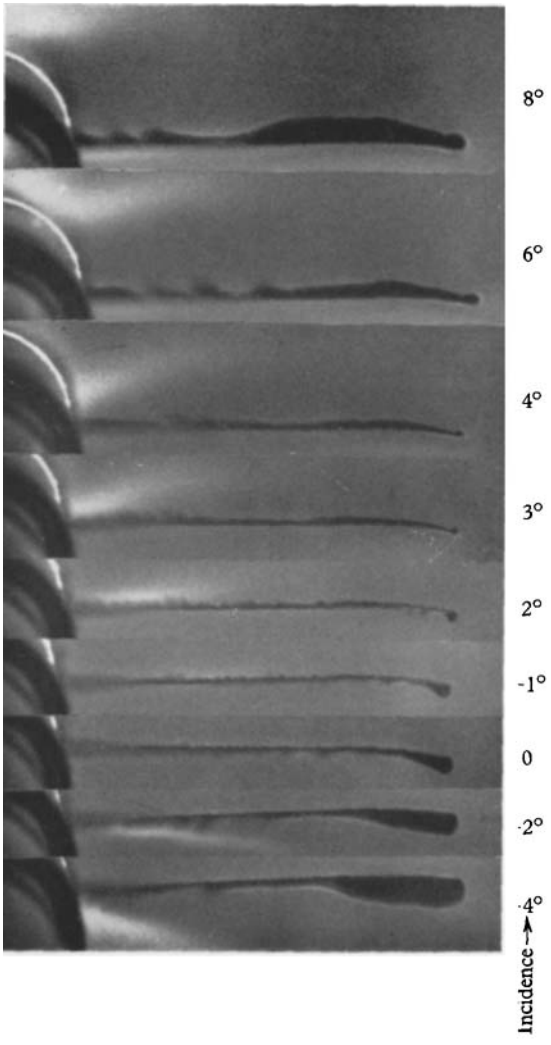

FIGURE 9, plate 1. Vapour-screen photographs of the flow behind a cambered delta wing at $M = 1{\cdot}51$.

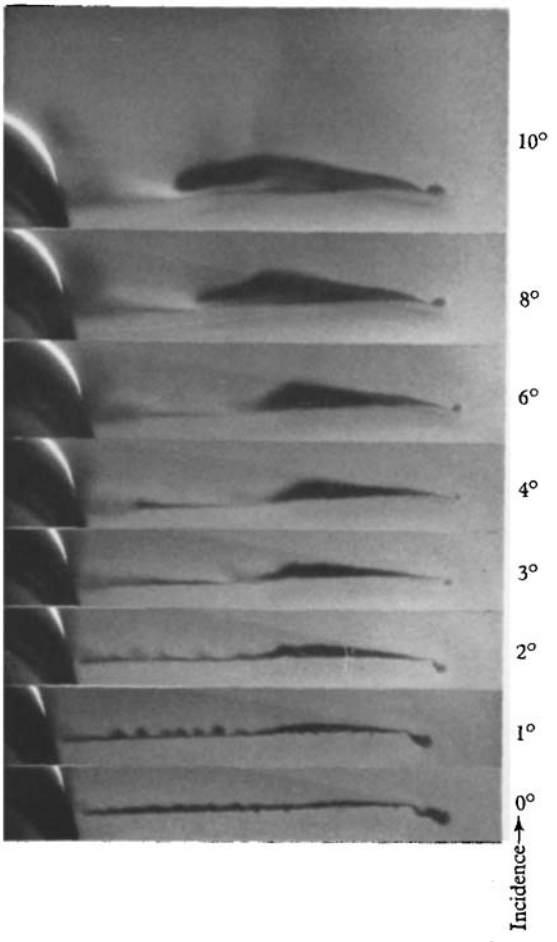

FIGURE 10, plate 1. Vapour-screen photographs of the flow behind a cambered delta wing at $M = 1{\cdot}88$ ($M_{\text{dry}} = 2{\cdot}00$).

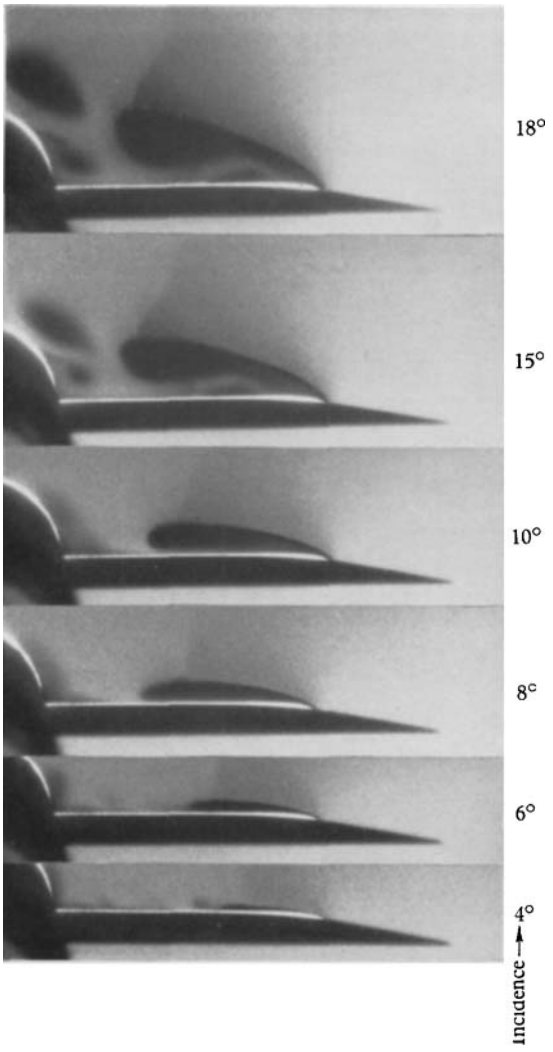

FIGURE 11, plate 2. Vapour-screen photographs of the flow over the upper surface of a plane wing at $M = 1{\cdot}75$ ($M_{\text{dry}} = 1{\cdot}81$).

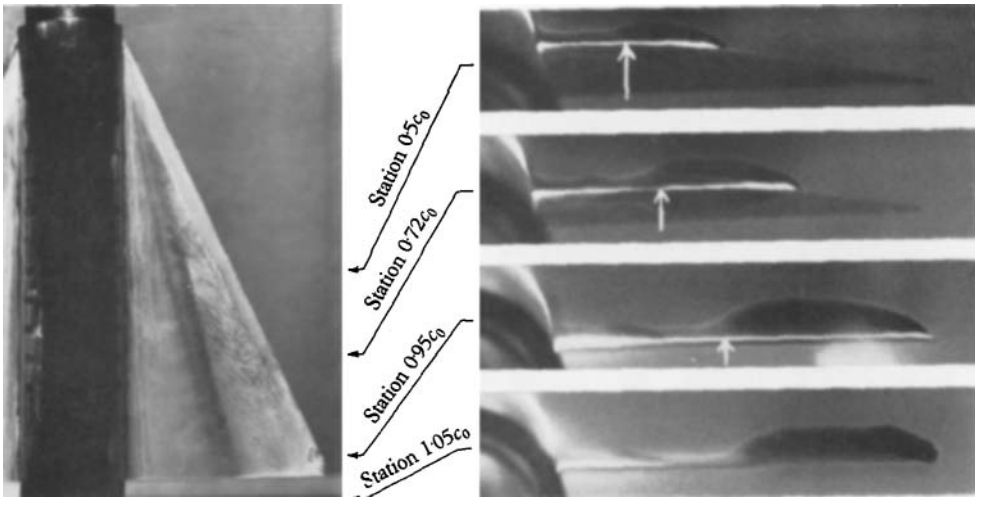

Arrows show position of reattachment, as given by oil-flow pattern

FIGURE 12, plate 3. Comparison of surface oil-flow and vapour-screen results on a plane wing at $M = 1{\cdot}51$, $\alpha = 8°$.

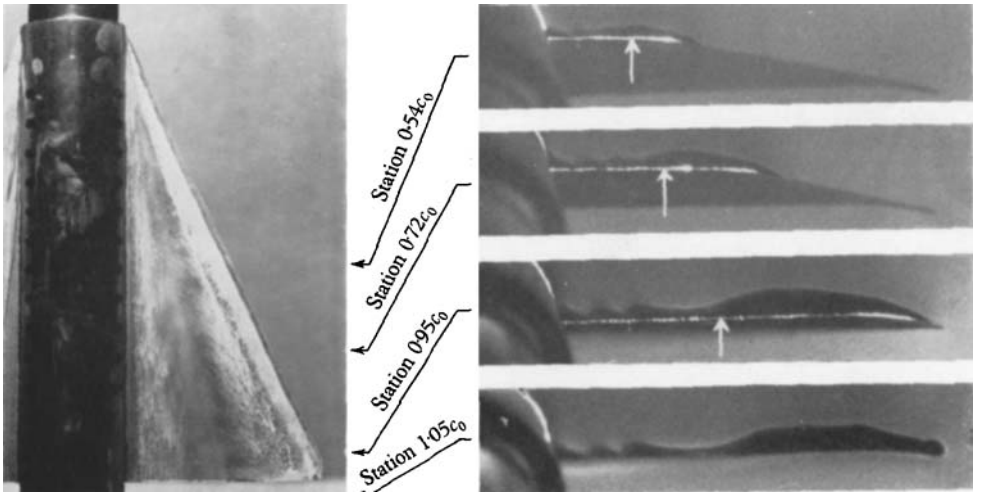

Arrows show position of reattachment, as given by oil-flow pattern

FIGURE 13, plate 3. Comparison of surface oil-flow and vapour-screen results on a cambered wing at $M = 1{\cdot}51$, $\alpha = 8°$.

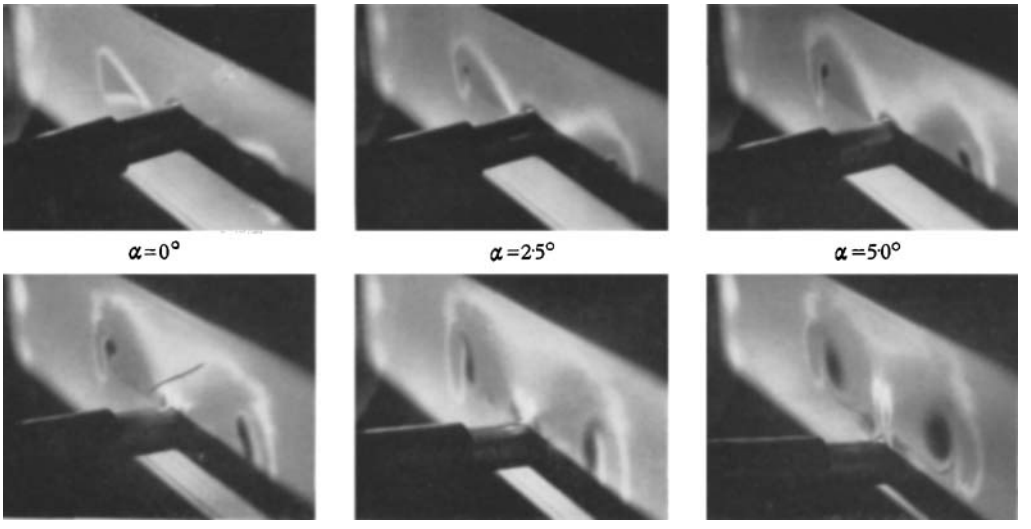

FIGURE 14, plate 4. Vapour-screen photographs taken at $M = 1{\cdot}32$ showing the 'blue line' phenomenon.

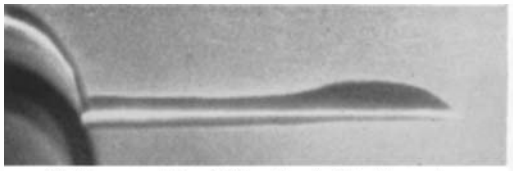

(i) Beam position $0{\cdot}05c_0$ ahead of trailing edge

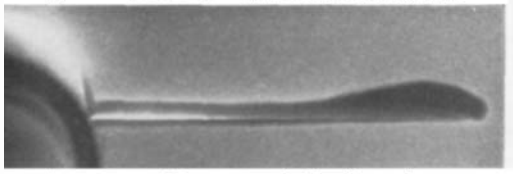

(ii) Beam position $0{\cdot}05c_0$ aft of trailing edge

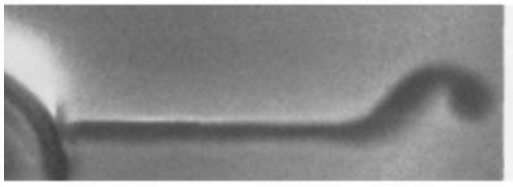

(iii) Beam position $0{\cdot}20c_0$ aft of trailing edge

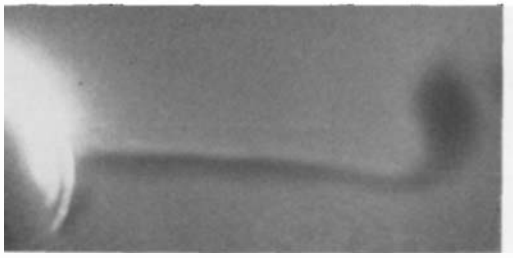

(iv) Beam position $0{\cdot}50c_0$ aft of trailing edge

FIGURE 15, plate 5. Vapour-screen photographs of the flow behind a delta wing at $M = 0{\cdot}85$, $\alpha = 4°$.

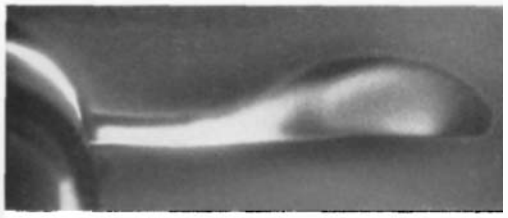

(i) Beam position $0{\cdot}05c_0$ aft of trailing edge

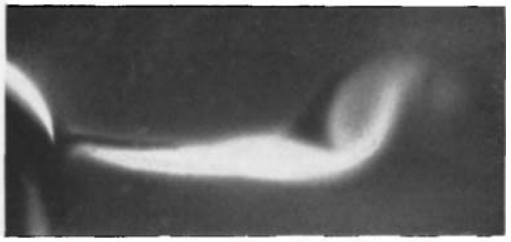

(ii) Beam position $0{\cdot}20c_0$ aft of trailing edge

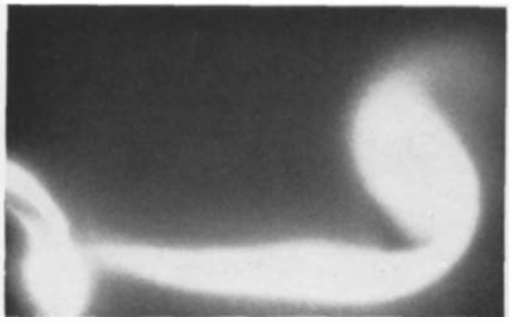

(iii) Beam position $0{\cdot}50c_0$ aft of trailing edge

FIGURE 16, plate 5. Vapour-screen photographs of the flow behind a delta wing at $M = 0{\cdot}85$, $\alpha = 8°$.

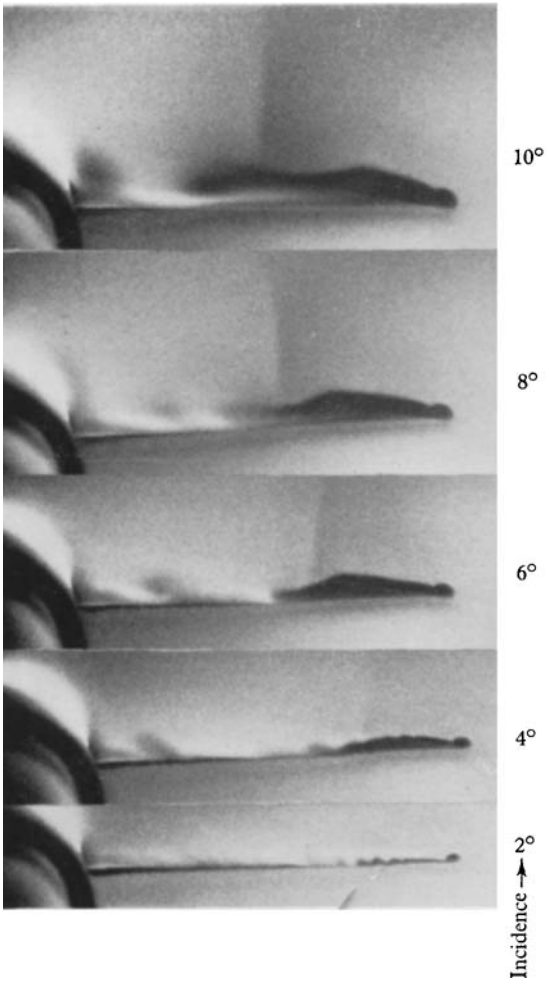

FIGURE 17, plate 6. Vapour-screen photographs of the flow just behind a delta wing, using carbon tetrachloride vapour, $M = 1{\cdot}96$.

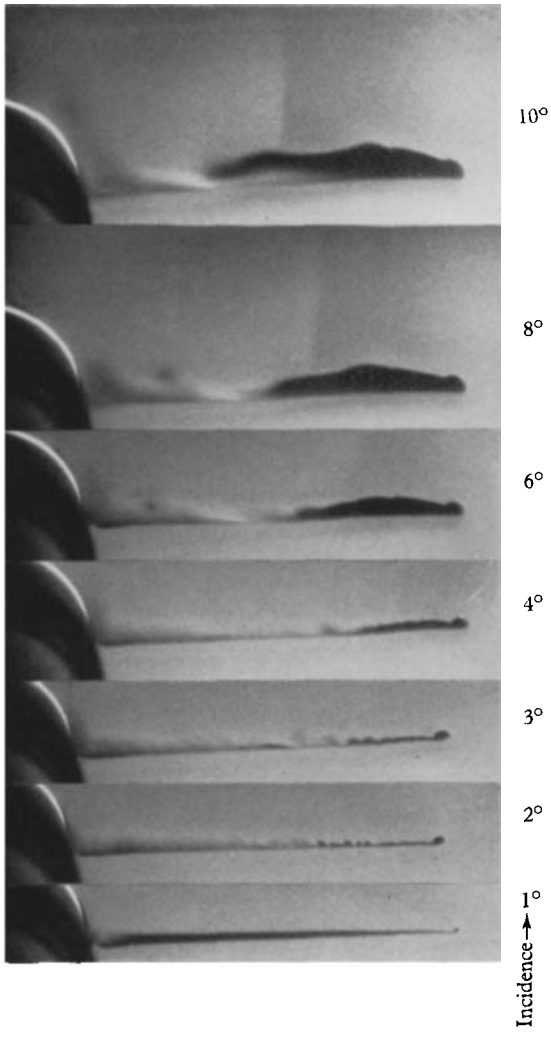

FIGURE 18, plate 6. Vapour-screen photographs of the flow just behind a delta wing, using water vapour, $M = 1{\cdot}88$ ($M_{dry} = 2{\cdot}00$).

number when a condensation shock is present in the nozzle. These theoretical values have been compared with the experimental results at a nominal Mach number of 2·00. Details of the calculations are also given in Appendix II, and the resulting values of M and p/p_{dry} have been added to figure 8. The calculated Mach number compares well with experiment at the lower humidities, but the theory overestimates the effect on Mach number as the humidity is increased. The 'step' in the experimental value of p/p_{dry} is not predicted, of course, but the mean rate of increase of static pressure with humidity is approximately correct.

5. Some typical vapour-screen photographs

The object of this section is to introduce a selection of typical vapour-screen photographs obtained with a series of wing-body combinations and to point out features of particular interest, but it is not proposed here to relate details of the flow revealed by these photographs to the general aerodynamic characteristics of the wings. A brief comparison is made, however, between some results obtained with the vapour-screen technique and the corresponding surface oil-flow patterns.

The models consisted of various delta wings mounted on the cylindrical part of an ogive-cylinder body. With the exception of that used in § 5.4, all the wings had a leading edge sweep of 65° and a thickness/chord ratio of 0·04. The extreme tips of the wings were removed, giving a taper ratio of 0·05, based on the root chord c_0 of the exposed wing. In all cases, free boundary-layer transition was permitted.

5.1. *Flow behind a cambered wing at two different Mach numbers*

A series of vapour-screen photographs showing the flow a distance $0{\cdot}05c_0$ behind the trailing edge of a cambered wing, at a number of different incidences, at actual Mach numbers of 1·51 and 1·88 ($M_{\mathrm{dry}} = 2{\cdot}00$) are presented in figures 9 and 10 (plate 1). The wing was of R.A.E. 101 section and cambered conically with respect to the apex of the gross wing to give an approximately elliptic spanwise loading at a lift coefficient of 0·15 at $M = 1{\cdot}57$. The photographs are reproduced at approximately $\frac{2}{5} \times$ model scale, and, from the point of view of technique, the most remarkable feature is the wealth of fine detail shown at low incidences, particularly at the higher Mach number. For example, at incidences of 3° and 4° a tiny vortex about 0·05 in. diameter can be clearly seen behind the extreme tip of the wing. With increase of incidence, this vortex grows in size and retains its roughly circular form, but at incidences less than 3° it becomes merged with a more complex flow originating on the undersurface of the wing in the tip region. At $M = 1{\cdot}88$, the flow near the tip at zero incidence is particularly intriguing.

Considerable differences in the flow over the upper surface of the wing may be observed between the two Mach numbers. At $M = 1{\cdot}51$, the flow appears to be completely attached to the wing surface up to 4° incidence, but at $M = 1{\cdot}88$ the photographs suggest that the flow is separating at incidences greater than about 1°. The design lift-coefficient for the camber corresponds to an incidence of approximately 4°, so it appears that the camber is successful in delaying leading

edge separation at Mach numbers near the design value. In general, the inboard end of the vortex region is more clearly defined at $M = 1{\cdot}88$, a rather thick wake from the inner half of the wing tending to obscure it at the lower Mach number. Also, the shape of the vortex region is more irregular at $M = 1{\cdot}88$, and there is a sudden increase in its spanwise extent between 6° and 8° incidence. This is probably due to the presence of a shock wave above the vortex, which can be seen in the photograph at 10° incidence. The shock is rendered visible by the change in density which occurs across it. At this Mach number, condensation is virtually complete, and, in the absence of extraneous forces on the fog particles, the number of particles per unit volume (and hence the amount of light scattered) will be directly proportional to the local air density. On passing through a shock wave the air undergoes a very rapid deceleration which the fog particles cannot follow owing to their much greater inertia. A relative velocity therefore exists between the air and the fog particles, but a simple calculation shows that this will be quickly reduced to zero by the action of viscosity and, a short† distance after passing through the shock, steady-state conditions will be re-established and the fog density will again be proportional to the local air density. The expansion over the leading edge causes a reduction in density and the screen darkens progressively from the leading edge towards the terminal shock. At the shock there is a sudden increase in density and the screen appears lighter due to the greater concentration of fog particles. The position of the shock therefore corresponds with the boundary between the darker and lighter regions, and some idea of the shock strength may be gained from the change in shade between the two regions. These effects are shown up much more clearly in figure 11 than in the present example.

A row of small black patches about 0·1 in. in diameter is visible behind the inner part of the wing at $M = 1{\cdot}88$ and 1° incidence (figure 10). It is believed that these are due to streamwise vortices in the boundary layer, caused by an instability of the three-dimensional shear flow in the region of the swept leading edge, the continuous transverse shear breaking down into a number of discrete vortices. They are probably also present at $M = 1{\cdot}51$, the wake behind the wing at 1° and 2° incidence having a rather jagged appearance, but are not nearly so distinct as at the higher Mach number.

White streaks or patches can be seen in all but one of the photographs at $M = 1{\cdot}51$, below the wing at negative incidences and above it at positive incidences. Originally these were thought to be of no account and due merely to light reflection from the body. However, it now seems certain that they are caused by additional condensation in regions of local flow expansion around the model. The matter is considered further in § 5.4. No condensation streaks were ever encountered at Mach numbers above 1·51.

† The relative velocity Δu at time t after passing through the shock wave is given approximately by $\Delta u = \Delta u_0 \exp[-18\mu t/d^2 w_L]$, where d is the diameter of the particle (assumed to be spherical), w_L its density (slug/ft.^{3}) and μ the viscosity of the air (lb.sec/ft.^{2}) For a spherical particle of radius 10^{-5} in., the relative velocity will be reduced to 1 % of its initial value in a time of approximately 5×10^{-6} sec, i.e. in a distance of less than 0·1 in. after passing through the shock wave.

5.2. *Flow over the upper surface of a plane wing at* $M = 1{\cdot}75$

Some photographs of the flow over the upper surface of a plane delta wing at an actual Mach number of 1·75 ($M_{\text{dry}} = 1{\cdot}81$) are shown in figure 11 (plate 2). The wing was of the same section (R.A.E. 101, 4 % thick) as before, but uncambered. The plane of the vapour screen was located approximately $0{\cdot}28c_0$ ahead of the trailing edge.

As mentioned previously, a shock wave is clearly visible above the wing vortex in this case, its strength increasing quite sharply with incidence above 10°.

An interesting change in the flow pattern occurs at an incidence of about 10°. Below this angle the flow separates from the leading edge, but later re-attaches, leaving a closed bubble containing a vortex on the wing surface. At higher incidences, however, a sheet of vorticity can be seen springing from the leading edge and rolling up into a vortex some distance above the surface. This vortex induces an outflow near the wing surface, but the outflow itself appears to separate and form a secondary vortex underneath the main vortex sheet.

Two further vortices close to the body at 15° and 18° incidence can be identified. The upper is one of a pair of body vortices caused by separation of the cross-flow over the forward part of the body at high incidence. The lower appears to be a wing-body junction vortex of the type described by Stanbrook (1959), which is caused by the interaction of the body boundary layer with the leading edge of the wing. A vortex sheet can be seen separating from the body at an angular position approximately 40° above the plane of the wing and rolling up to form this vortex.

5.3. *Comparison of surface oil-flow and vapour-screen techniques on two wings at* $M = 1{\cdot}51$

Figures 12 and 13 (plate 3) have been prepared so that details of the flow shown by the vapour screen may be easily compared with those given by surface oil-flow patterns. Both of these figures show vapour-screen photographs obtained just behind the trailing edge and at three stations on a wing at 8° incidence, at a Mach number of 1·51, together with a photograph of the oil-flow pattern (obtained using a mixture of heavy oil and titanium dioxide with a trace of oleic acid as anticoagulant) at the same conditions. The two wings used were the plane and cambered 4 %-thick delta wings referred to above, figure 12 (plate 3) showing the results for the plane wing.

The only significant differences shown by the oil-flow patterns are that, on the cambered wing, separation occurs slightly further aft of the leading edge, and the reattachment line is slightly curved. However, the vapour-screen pictures show that the height and area of the vortex region and the angle at which the flow separates from the wing surface are appreciably greater in the case of the plane wing. The vapour-screen photographs on the cambered wing also show what appear to be three small vortices in the boundary layer inboard of the main leading edge vortex. There is no indication of these vortices in the oil-flow pattern, and their origin is obscure. They may also be seen in the photograph at 6° incidence in figure 9 (plate 1), but there is no similar effect on the plane wing.

The position of reattachment may be obtained with considerable accuracy

from the oil-flow patterns, and this point has been marked on the vapour-screen photographs for the three stations on the wing. Close examination of the vapour-screen photograph at the $0{\cdot}95c_0$ station on the plane wing reveals that the flow immediately above the wing may be divided into three parts—a black region over the outer part of the wing, shaped roughly like a segment of a circle and which appears to be devoid of fog particles, a grey region which extends as a narrow band above the wing surface from the inboard end of the black region to the body, and a thin bright line running from the body to the leading edge of the wing which forms an upper boundary to both the grey and black regions. It appears that the point of reattachment coincides with the inboard end of the black region, so it is not unreasonable to suppose that the size and shape of this region correspond fairly closely with those of the actual leading edge vortex. At the other vapour-screen stations, and on the cambered wing, it is virtually impossible to distinguish between these two regions and they appear as a single dark region, but in general reattachment occurs at a spanwise position near the point of inflexion of the bright line surrounding the dark region. This line, and the dark region over the inner part of the wing where the flow is attached, are characteristic of results obtained at Mach numbers up to 1·51. Above this speed, as shown in figures 10 and 11 (plates 1 and 2), the inboard end of what is assumed to be the leading-edge vortex is quite sharply defined and there is no contiguous dark band over the inner part of the wing. In § 6, it is suggested that this difference is due to the smaller size of the fog particles at the higher Mach numbers.

5.4. *An interesting phenomenon at* $M = 1{\cdot}32$

At an early stage of the present investigation, when fog formation at different Mach numbers was being studied, a test was being performed at a Mach number of 1·32. As usual during these tests, a model was mounted in the tunnel so that the quality of the vapour-screen picture could be judged. As the beam of light was being moved further aft behind the model, a most interesting phenomenon occurred. In addition to the normal black patches on the screen caused by vortices from the wing, a symmetrical pattern of bright blue lines developed, which appeared to emanate from the centre of the screen and become entwined with the wing vortices. It is not possible in a black and white reproduction to recapture fully the striking nature of this effect—a pattern in blue and black on an iridescent background half green, half violet—but the photographs in figure 14 (plate 4), which were originally taken on colour film, give a good impression of the phenomenon. The model used was similar to those described previously, but fitted with a 55° leading-edge-sweep delta wing of R.A.E. 101 section, 6 % thick. The plane of the vapour screen was located approximately 9·5 in. (1·2 wing-root chords) behind the trailing edge of the wing. The blue lines were present even at zero incidence, when they formed a roughly triangular shape behind each wing panel, with the apex towards the body. Their shape changed as incidence was applied, the upper side of the triangle becoming curved and the lower side swinging round as if to unite with the wing vortex.

The lines from the body became rather diffuse by about 7° incidence, but two blue lobe-like shapes appeared in the screen on top of the sting on which the

model was mounted. With further increase of incidence the vertical height of the lobes increased and their tips assumed a whitish tinge. It was found that on moving the light beam towards the model the main pattern of blue lines became fainter, and they disappeared completely when the beam was about 6 in. from the trailing edge of the wing. The blue lobes above the body at high incidence persisted, however, until the beam was ahead of the trailing edge.

At the time, the origin of the blue lines was the subject of much speculation. No quite similar effect could be found at other Mach numbers, although at $M = 1{\cdot}41$ and 1·51 blue lobes could be seen at high incidence when the light beam was behind the wing trailing edge. The matter was finally resolved when a long, slender body of revolution was being tested at a Mach number of 1·41. The light beam was located towards the rear of the body and the model happened to be at a considerable incidence while water was being added to the tunnel. It was discovered that two faint blue lobes could be seen above the body in the path of the light beam before the humidity was sufficient to produce a visible vapour screen. It was therefore concluded that the blue coloration was due to local condensation, caused by flow expansion in the immediate vicinity of the model.

This explanation further confirms the mechanism of condensation proposed in § 4.5. No blue lines were detected under any conditions at a Mach number greater than 1·51. However, condensation occurs at a condensation shock above this Mach number and the flow is not supersaturated after the shock. It is therefore not possible for additional condensation to occur at the model. At Mach numbers up to and including 1·51, it is believed that the primary condensation occurs on foreign nuclei and only a fraction of the water vapour present in the working section is condensed out. The flow is still well supersaturated and secondary condensation may occur in any region where expansion of the flow is sufficient to raise the local level of supersaturation above the critical value. In view of the comparatively small size of the regions causing additional condensation, it is probable that such condensation occurs on self-generated nuclei. This implies that there may be condensation shocks in the vicinity of the model, but it is considered that the influence of these shocks on the overall flow around the model is likely to be very small.

6. The formation of the vapour-screen picture

The mechanism by which a shock wave is rendered visible by the vapour screen has already been discussed in § 5.1. We will now consider briefly other ways in which the uniform distribution of fog particles may be disturbed sufficiently to produce noticeable changes in the amount of light scattered by the fog.

A priori, two causes would appear to be responsible—heating, so that the fog particles tend to evaporate, and failure of the fog particles to follow the motion of the air in regions of flow curvature or acceleration due to their much greater inertia.

Heating due to compression will only occur to a significant extent near a stagnation point or through a strong shock wave, but in these circumstances effects due to droplet inertia will be much more important. Other regions in which the temperature may be considerably above the stream temperature are the boundary layer and regions of low mean velocity after boundary-layer

separation. However, Crane (1959) has deduced from measurements of recovery temperature that in a laminar boundary layer no re-evaporation occurs and that with a turbulent boundary layer re-evaporation is only partial. It therefore appears that localized temperature effects are not important in the formation of the vapour-screen picture, except possibly in the case of wakes behind wings or bodies at low incidence.

Effects due to droplet inertia occur in two distinct regions—the region near the leading edge of a wing or the front stagnation point of a body, and regions of vortical flow. The behaviour of water droplets in the neighbourhood of the leading edge has for long been of interest in connexion with the problem of icing. Unfortunately the equations governing the motion of the droplets cannot be solved in closed form, but numerical solutions have been obtained for a number of different aerofoils at subsonic speeds. According to Glauert (1940), the be haviour of the droplets depends on the dimensionless inertia parameter k, defined as $k = \frac{2}{9}w_L r^2 U/\mu c$, where w_L is the density of the droplet of radius r, μ the viscosity of the air, U the free stream velocity and c the chord of the aerofoil. For a particular aerofoil at a given incidence, there is a critical value of k. If k is less than the critical value, no droplets strike the aerofoil, but if k exceeds the critical value, all the droplets in a certain stream-tube an infinite distance ahead of the leading edge strike the aerofoil. Both the width of the stream-tube and the area of impingement increase with k. This effect may explain the dark bands over the inner parts of the wings shown in the vapour-screen photographs at $M = 1{\cdot}51$ (figures 12 and 13, plate 3) and mentioned in § 5.3. At $M = 1{\cdot}51$, when the radius of the fog particles is about 3×10^{-5} in., k is of order $0{\cdot}1$. The radius is not known with any degree of certainty at higher Mach numbers, but it is probably not greater than 10^{-5} in., so that k is of order of $0{\cdot}01$. Thus at $M = 1{\cdot}51$, droplets are likely to impinge on the nose of the aerofoil (where they presumably evaporate) and so the air immediately above the surface is devoid of fog particles, but at higher Mach numbers the lower value of k greatly reduces this tendency, and may even eliminate it completely.

There is little doubt that all the above-mentioned effects are of quite minor importance in the formation of the vapour-screen picture compared with the influence of vortices. The radial acceleration produced by circulatory flow exerts a powerful centrifuging action on the fog particles and they are rapidly swept from the centre of the vortex. A point of great interest, but one which cannot be definitely resolved from the present tests, is the relationship between the size and shape of a region clear of fog with those of the vortex causing it. The boundary of such regions is invariably well-defined, but can a vortex possess such a boundary? This difficulty is removed if it is remembered that the vortices under consideration here are quite different from the classical concept of an irrotational vortex in an inviscid fluid. They are essentially three-dimensional, rotational and viscous, produced by the accumulation of vorticity shed from lines of boundary-layer separation near the leading edge of the wing or from the body. From an examination of large numbers of photographs, it is suggested that the black regions shown on the vapour screen are caused by these rotational vortex cores, and the boundary of the region is a fairly close approximation to the

boundary between the core and the outer irrotational flow field, but a detailed survey of flow conditions is necessary before this can be definitely established.

7. The vapour screen at subsonic speeds

All previous applications of the vapour-screen technique have been restricted to supersonic speeds, but there are no fundamental reasons why the method should not be employed at the higher subsonic and transonic speeds provided a sufficiently large drop in temperature between the settling chamber and working section can be achieved. Some tests were therefore made to examine vapour-screen production under these conditions.

Ideally, the use of a slotted or porous-wall working section is necessary for such an investigation, but this was impossible in the present instance, since the transonic working section of the 3 ft. tunnel does not possess any apertures suitable for the passage of the light beam. As an alternative, a flat top liner was used in the supersonic working section, converting it, in effect, to a subsonic tunnel. This presented no serious disadvantage since the main purpose of these tests was to determine the lowest subsonic Mach number at which the vapour-screen technique could be usefully employed.

The first test was made at $M = 0{\cdot}80$ with a total pressure of 20 in. Hg and a total temperature of approximately 40 °C. The same procedure was followed as in previous tests at supersonic speeds. It was found necessary to inject some 15 gallons of water before an adequately dense vapour screen was produced, but the screen tended to thin once the flow of water into the tunnel ceased. This was because the air was saturated at stagnation conditions and condensation occurred on the tunnel walls and in other cool parts of the circuit. The trouble was cured by injecting water continuously into the tunnel at a rate sufficient to make up for this condensation. However, in spite of the screen appearing reasonably satisfactory when viewed from the side of the tunnel, attempts to photograph it from downstream were unsuccessful, the picture being almost completely obscured by dense white patches caused by local condensation around the model. An impression was gained that the dropletes forming the fog were considerably larger than those at higher speeds, and globules of water could frequently be seen streaming over the surface of the model and collecting at the trailing edge of the wing and the base of the body.

A second test at $M = 0{\cdot}85$, with the same total temperature and pressure as before, proved more successful. About 10 gallons of water were required to produce an adequate vapour screen, which had the same iridescent character as at the lower supersonic Mach numbers. Some typical results are presented in figures 15 and 16 (plate 5), which show the rolling-up of the vortex sheet at various distances behind a 65° leading-edge-sweep delta wing at incidence of 4° and 8°. At 4° incidence, the results are quite normal and the edges of the vortex sheet are clearly defined, but at 8° it is possible that the higher velocities inside the vortex region caused a drop in temperature sufficient to cause condensation to occur at a greater rate than the fog particles could be swept from the core of the vortex. At the most rearward station there is a complete 'image reversal' effect, the vortex sheet appearing white on a relatively dark background.

The conclusion drawn from these tests is that the lowest Mach number at which the vapour-screen technique is practicable is approximately 0·85, but this may be rather too low if the shape of the model or the range of incidence over which it is to be examined is such that flow expansion around the model causes excessive local condensation.

8. Use of liquids other than water for vapour-screen production

An undesirable feature of the vapour-screen technique is that, at Mach numbers greater than about 1·6, a condensation shock occurs upstream of the working section at a humidity less than that necessary to produce a satisfactory vapour screen. This shock reduces the actual Mach number below the nominal for the nozzle, increases the static pressure and may produce flow disturbances in the working section.

The condensation shock is caused by the sudden liberation of the latent heat of evaporation when vapour condenses into liquid, and to first order the strength of the shock and its effect on the flow are directly proportional to the amount of heat added per unit mass of air. It is possible to reduce the strength of the shock, for a given degree of condensation, by increasing the total pressure, but the improvement available is strictly limited by the design of the tunnel. A more fundamental approach lies in the use of liquids which have a lower latent heat of evaporation than water. Now the latent heat h and molecular weight m are related by $hm = CT_b$ (Trouton's Rule), where T_b is the boiling temperature and C is a constant which has the value 21 for substances which are unassociated in both the liquid and vapour states. It therefore follows that, in general, a liquid of high molecular weight will have a low latent heat of evaporation.

The properties desirable in a liquid whose use is contemplated for vapour-screen production can be summarized as follows. It must be (*a*) chemically stable, (*b*) of high molecular weight, (*c*) of low toxicity, (*d*) non-corrosive, (*e*) non-inflammable, (*f*) preferably readily available commercially, and (*g*) have a saturated vapour density such that (i) a sufficient quantity can be introduced before reaching saturation under stagnation conditions, and (ii) an excessive quantity is not required to produce saturation at the working section static temperature. The number of liquids satisfying all these conditions is quite small and the most promising appear to be a group of organic chlorine compounds, carbon tetrachloride, CCl_4, tetrachlorethylene, C_2Cl_4, tetrachloroethane, $C_2H_2Cl_4$, and pentachloroethane, C_2HCl_5.

It was decided to carry out a test using carbon tetrachloride, as bulk supplies were immediately available. The relevant physical properties of carbon tetrachloride and water are compared in the table below:

	CCl_4	Water
Specific gravity at 0 °C	1·63	1·00
Boiling point at 760 mm. Hg, °C	76·8	100
Freezing point, °C	−23	0
Molecular weight	154	18
Latent heat of evaporation (C.H.U./lb.)	46·4 at 76·8 °C	595 at 0 °C
Latent heat of fusion (C.H.U./lb.)	4·16	79·7
Specific heat of liquid (C.H.U./lb. °C)	0·20	1·00

The test was made at a nominal Mach number of 2·00, with a total pressure of 9·00 in. Hg, and a total temperature of approximately 47 °C. The air was dried as thoroughly as possible before admitting any carbon tetrachloride. The liquid was injected into the diffuser one pint at a time and the working section static pressure measured. Condensation could first be detected visually after 4 pints had been added, and by the time 8 pints were added the vapour screen was adjudged to be sufficiently dense to permit satisfactory photographs to be taken. The screen appeared a deep bluish-violet colour viewed from the side of the tunnel.

The increase in static pressure, p/p_{dry}, with quantity of carbon tetrachloride in the tunnel is shown in figure 8. Between 2 and 6 pints, the mean slope is approximately one-seventh of that when using water, which is roughly the ratio predicted by simple theory. With 8 pints in the tunnel, $p/p_{\text{dry}} = 1{\cdot}040$ and the actual Mach number = 1·96, approximately. Using 6 pints of water at the same total temperature and pressure, $p/p_{\text{dry}} = 1{\cdot}205$ and the actual Mach number = 1·88. It is thus seen that the severity of the condensation shock may be greatly reduced by the use of carbon tetrachloride in place of water.

Some photographs of the flow just behind the trailing edge of a 65° leading-edge-sweep delta wing with a 4 %-thick biconvex section obtained using the carbon tetrachloride screen are presented in figure 17 (plate 6) with the corresponding photographs using water in figure 18 (plate 6) for comparison. The general quality of the photographs is similar in the two cases, and the most noticeable difference is that, with the carbon tetrachloride screen (and higher working section Mach number), the shock wave visible on top of the vortex at incidences of 6°, 8° and 10° is located approximately 6 % of the semi-span further inboard.

9. Conclusions

The vapour-screen technique affords a simple and practical method of flow visualization at supersonic speeds, and, with some limitations, may even be employed at Mach numbers as low as 0·85. It is capable of providing much useful information about the flow over and behind wings and bodies, such details as vortices, vortex sheets, lines of flow separation or reattachment and shock waves being rendered clearly visible.

A high standard of temperature uniformity over the working section is essential if good results are to be obtained, and to achieve such a standard in the 3 ft. tunnel entailed shutting off the aftercooler and running at reduced total pressure at a total temperature of 40–50 °C. Close control of the humidity is also necessary, the procedure used consisting of running the tunnel with the driers in circuit to reduce the humidity to a low level (corresponding to a frost-point of about −40 °C), switching off the driers, and then injecting measured quantities of water into the diffuser.

The humidity required to produce an optimum density of fog in the working section (from the point of view of obtaining the best photographs of the vapour-screen picture) is fairly critical, and is affected by Mach number, total pressure and temperature. With a total pressure of 12 in. Hg and a total temperature of 45 °C, it was found that the optimum humidity reached a minimum value at

about $M = 1{\cdot}6$, increasing very rapidly below this Mach number and rather slowly above it. At Mach numbers up to and including 1·51 (with the above conditions of temperature and pressure), the screen had an iridescent appearance due to diffraction of the light beam by the fog particles. An estimate of the size of the particles based on the position of the coloured diffraction bands at $M = 1{\cdot}41$ gave the radius as approximately 3×10^{-5} in., corresponding to a particle density of about 10^7 per in.^{3}. In this Mach number range it was possible to obtain sufficient condensation to form a satisfactory vapour screen without affecting either the working section static pressure or Mach number, and it is suggested that condensation occurred on foreign condensation nuclei.

At higher Mach numbers, the vapour screen was pale blue in colour and the fog probably consisted of ice crystals rather than water droplets. Condensation occurred at a condensation shock in the nozzle upstream of the working section, which increased the static pressure and decreased the Mach number in the working section. Tests at a nominal Mach number of 2·00 showed that the variation of Mach number and static pressure with humidity agreed well with the first-order theory of Monaghan (1956) at low humidities, but the theory was unduly pessimistic with regard to the effect on Mach number in the range of humidity necessary to produce a satisfactory vapour screen.

The quality of the vapour-screen picture was generally superior at Mach numbers above 1·51, this being ascribed to the smaller size of the fog particles due to the different mechanism of condensation. At lower speeds the flow in the working section was still supersaturated, and patches of additional local condensation caused by flow expansion around the model were frequently observed. Under certain conditions, and particularly at $M = 1{\cdot}32$, these condensation patches or streaks formed an intricate pattern superimposed on the normal vapour-screen picture.

The adverse effects of the condensation shock on the flow at the higher Mach numbers may be alleviated by the use of liquids with a lower latent heat of evaporation than water. A test at a nominal Mach number of 2·00 showed that a vapour-screen picture of a quality comparable with that obtained using water vapour could be produced with carbon tetrachloride vapour. The actual Mach number in the working section was 1·96, compared with a value of 1·88 when using water vapour.

Appendix I: The mechanism of condensation at Mach numbers less than 1·5

It was suggested in § 4.5 that, at Mach numbers up to and including 1·51, condensation occurs principally on foreign nuclei rather than on nuclei generated spontaneously in the supersaturated vapour by random molecular aggregation. Since this is at variance with the commonly accepted view of the mechanism of condensation in wind tunnels at supersonic speeds, the matter will be considered in some detail.

We will first attempt to show that the size of the droplets, as estimated from observation of the coloured diffraction bands at $M = 1{\cdot}41$, is of the same order as that predicted theoretically, on the assumption that a droplet starts to form

around a condensation nucleus at the point in the nozzle where the water vapour is just saturated and continues to grow on its passage down the nozzle by a process of diffusion of water vapour on to the surface of the droplet. To perform this calculation it is necessary to make an assumption concerning the variation of the density of the uncondensed water vapour along the length of the nozzle. This variation is known when there is no condensation, but is indeterminate once condensation has started, unless the number of droplets is also known. Consequently, the calculated value of the droplet radius must be regarded as a rough estimate only, but its order of magnitude should be correct.

The equation governing the rate of growth of a droplet in a moving airstream is given by Oswatitsch (1941) as

$$r\frac{dr}{dx} = \frac{w - w_{\text{sat.}}}{w_L}\frac{D}{u},$$

where r = radius of the (spherical) droplet,
x = axial co-ordinate,
w = density of the uncondensed vapour surrounding the droplet,
$w_{\text{sat.}}$ = density of saturated vapour at the surface of the droplet,
w_L = density of the liquid forming the droplet (= 62·4 lb./ft.^{3}),
D = coefficient of diffusion of water vapour in air,
u = velocity of the airstream.

This equation may be integrated to give

$$r^2 = 2\int_0^l \frac{w - w_{\text{sat.}}}{w_L}\frac{D}{u}\,dx,$$

where l is the distance travelled by the drop since its formation. In the case of flow through a supersonic nozzle, all the quantities on the right-hand side of this equation (with the exception of w_L) are functions of x, but it may be shown that, in the Mach number range we are concerned with here (1·0–1·5 approximately), the ratio D/u is very nearly constant, so that

$$r^2 = \frac{2}{w_L}\left(\frac{D}{u}\right)\int_0^l (w - w_{\text{sat.}})\,dx.$$

Unfortunately, the variation of $(w - w_{\text{sat.}})$ with distance along the nozzle is indeterminate, but we can obtain a rough estimate of the droplet radius by assuming a simple, plausible variation of $(w - w_{\text{sat.}})$ with x. For example, suppose we assume that $(w - w_{\text{sat.}})$ increases linearly with x. We then have, for the radius, $r = \{Dl[w - w_{\text{sat.}}]_l/uw_L\}^{\frac{1}{2}}$.

Let us consider the case of $M = 1{\cdot}4$, with a total pressure p_t of 12·0 in. Hg, a total temperature T_t of 45 °C, and with 12 pints of water added to the tunnel. The flow becomes just saturated at a point in the nozzle where the local Mach number is 0·98, and in accordance with our initial hypothesis it will be assumed that condensation starts from this point. The distance from this point to the centre of the working section, i.e. the distance l, is 9·5 ft. The coefficient of

diffusion D is given by Oswatitsch as $D = 0{\cdot}000225(T/273)^{1{\cdot}86}(30/p)$ ft.^{2}/sec, so that the mean value of D/u between $M = 1{\cdot}0$ and $M = 1{\cdot}4$ is $0{\cdot}93 \times 10^{-6}$ ft. for the conditions specified above.

The working section static temperature is -43 °C under isentropic conditions, and from figure 5 the corresponding density of saturated water vapour, $w_{\text{sat.}}$, is $5{\cdot}1 \times 10^{-6}$ lb./ft.^{3}. If we assume that half of the water vapour has condensed at the working section, the actual density of the uncondensed vapour is 73×10^{-6} lb./ft.^{3}. Inserting these values in the equation for r gives a droplet radius of $3{\cdot}8 \times 10^{-5}$ in., which is considered to be in quite reasonable agreement with the value of 3×10^{-5} in. estimated from observation of the coloured diffraction bands at $M = 1{\cdot}41$.

If we again assume half of the vapour to have condensed by the time the working section is reached, and taking the droplet radius as 3×10^{-5} in., the number of droplets in this case works out at 10^7 per in.^{3}. Therefore if condensation is occurring on foreign condensation nuclei, there must be at least this number of nuclei present in the air in the tunnel. At first sight this may appear to be an excessive number, but in fact is less than the number that have been measured in ordinary room air, and is of the same order as that found in an urban atmosphere. We thus conclude that the size and number of the droplets are not inconsistent with the proposition that condensation is occurring on foreign nuclei.

The theory of molecular nucleus formation is based on the kinetic theory of gases, and whilst complicated in detail, the results may be expressed comparatively simply. It is found that the rate of nucleus formation per unit volume depends on two parameters—the temperature and the ratio of the actual vapour pressure to the saturation vapour pressure, i.e. the supersaturation.

Burgess & Seashore (1951) have presented a chart of the rate of nucleus formation as a function of the supersaturation and stream temperature. At a Mach number of 1·4, with a total temperature of 45 °C and a static temperature of -43 °C, the relation between the supersaturation S and the rate of nucleus formation J (expressed as the number of nuclei generated in 1 in.^{3} of vapour while travelling a distance of 1 ft.) is as follows:

J	1	10^2	10^4	10^6	10^8	10^{10}	10^{12}
S	10·0	11·3	12·9	15·2	18·2	22·2	28·7

Thus the number of self-generated nuclei becomes of the same order as the number of droplets estimated to be present when a 16-fold supersaturation is attained. Referring to figure 4, it is seen that at $M = 1{\cdot}4$ condensation is first detectable in the working section at just this level of supersaturation. This might be considered excellent agreement between theory and experiment and to justify fully the assumption that in supersonic tunnels condensation is due to self-generated nuclei, but there are reasons for supposing that this agreement is fortuitous. If the supersaturation is increased by increasing the initial humidity a comparatively small amount, the rate of nucleus formation increases by several orders of magnitude, which would cause a sudden and complete collapse of the supersaturated state, i.e. a condensation shock. The experimental results do not

reveal the existence of any such shock in the Mach number range under consideration until humidities rather greater than that found necessary to produce a satisfactory vapour screen. There is also the evidence (§ 5.4) that the flow in the working section is still well supersaturated, although this is not the case at the higher Mach numbers, when condensation does occur at a condensation shock.

The molecular nucleus-formation theory disregards an important factor when applied to the flow in wind tunnels. This is the effect of the temperature gradient along the nozzle, which has been discussed by Smolderen (1956). Suppose we express the supersaturation not as the ratio of the actual pressure of the supersaturated vapour to the saturated vapour pressure, but as the 'adiabatic supercooling'. This is defined as the difference in temperature between the point in the nozzle at which the vapour is just saturated, and the actual vapour temperature. At $M = 1{\cdot}4$ and with a 16-fold supersaturation in the working section (where the static temperature is $-43\,^{\circ}\mathrm{C}$), the flow is just saturated at a point in the nozzle where the local static temperature is $-12\,^{\circ}\mathrm{C}$. Thus the adiabatic supercooling is 31 °C, which is a fairly typical value of the supercooling necessary to cause condensation, as given by this theory. However, Smolderen presents evidence that even in large tunnels condensation effects are rarely encountered with an adiabatic supercooling of less than 40 °C and in a small tunnel this may rise to 60 or 70 °C or more. A change in the adiabatic supercooling from 31 to 40 °C represents an increase of over 100 % in the supersaturation.

It is therefore considered that at the lower supersonic speeds the weight of evidence is against the theory that condensation is due to self-generated nuclei, and its appears that foreign nuclei are primarily responsible. It must be emphasized, however, that this conclusion is only valid for the 3 ft. tunnel for the particular conditions of pressure and temperature under which it was operated, and will not necessarily be true in general. For example, a reduction in total temperature while keeping the stagnation humidity constant will have little effect on the rate of growth of a droplet forming around a foreign condensation nucleus, but it will increase the adiabatic supercooling, thus greatly increasing the likelihood of self-generated nuclei dominating the condensation process. It might well be found that at a total temperature of 15 °C the presence of foreign nuclei is significant only at Mach numbers less than about 1·2.

The effect of a reduction in tunnel size is interesting. The shorter distance between throat and working section is obviously unfavourable to the growth of droplets on foreign nuclei, which tends to increase the supersaturation of the uncondensed vapour, thus increasing the probability of molecular nucleus formation. However, the steeper temperature gradient in the shorter nozzle increases the adiabatic supercooling necessary to cause condensation. It is therefore difficult to predict the effect of a reduction in tunnel size on the mechanism of condensation, but it is certain that to produce, at the same Mach number and total pressure, a vapour screen of equal density in a small and in a large tunnel, then the stagnation humidity must be greater in the former case than in the latter.

Appendix II: Estimation of working-section Mach number and static pressure when a condensation shock is present in the nozzle at $M_{\text{dry}} = 2{\cdot}0$

Monaghan (1956) has derived the following approximate relations for the working section static pressure and Mach number when a condensation shock is present in the nozzle:

$$\frac{p}{p_{\text{dry}}} \simeq 1+\frac{1}{2}\left[\frac{\gamma M_{\text{dry}}^2}{M_{\text{dry}}^2-1}(1+\gamma M_1^2)-\gamma M_1^2\right]\frac{q}{c_p T_t},$$

$$\frac{M}{M_{\text{dry}}} \simeq 1-\frac{1}{2}\left[\frac{(1+\gamma M_1^2)\{1+\tfrac{1}{2}(\gamma-1)M_{\text{dry}}^2\}}{M_{\text{dry}}^2-1}\right]\frac{q}{c_p T_t},$$

where M_1 = Mach number just ahead of the condensation shock,
q = heat input per unit mass of gas (C.H.U./lb.),
c_p = specific heat of air at constant pressure (0·24 C.H.U./lb. °C),
T_t = total temperature of the air ahead of the shock (°K).

Before these expressions can be evaluated it is first necessary to estimate the value of M_1, and this has been done by assuming a constant adiabatic supercooling of 50 °C (see Appendix I), which corresponds to condensation effects being just detectable at a frost-point of − 37 °C with an initial total temperature of 47 °C. It is assumed that the wet air expands isentropically through the nozzle until condensation occurs, and that the density and temperature of the small quantity of water vapour present vary directly as that of the much larger mass of air. The temperature $T_{\text{sat.}}$ at which the vapour is just saturated may then be found for any stagnation vapour density by cross-plotting on figure 5. With a total temperature T_t of 47 °C, and assuming an initial vapour density of $0{\cdot}7 \times 10^{-5}$ lb./ft.^{3} (corresponding to a frost-point of − 40 °C) for the 'dry' tunnel, we can calculate M_1 as follows. W is the quantity of water added to the tunnel, w_t the density of the water vapour in the settling chamber and T_1 the temperature just ahead of the condensation shock.

W (lb.)	w_t (lb./ft.^{3})	$T_{\text{sat.}}$ (°C)	T_1 (°C)	T_1/T_t	M_1
2·5	$6{\cdot}3 \times 10^{-5}$	− 24	− 74	0·622	1·74
5·0	$11{\cdot}8 \times 10^{-5}$	− 18	− 68	0·641	1·67
7·5	$17{\cdot}3 \times 10^{-5}$	− 13	− 63	0·657	1·62

In calculating q it has been assumed that all the water vapour is condensed out at the shock, and that ice crystals rather than water droplets are formed, so a total latent heat h of 690 C.H.U./lb. has been used. With a total pressure of 9 in. Hg, the density ρ_t of the air in the settling chamber is 0·0218 lb./ft.^{3}. Since $q = hw_t/\rho_t$, we have finally:

W (lb.)	M_1	$q/c_p T_t$	M	p/p_{dry}
2·5	1·74	0·026	1·92	1·07
5·0	1·67	0·049	1·86	1·13
7·5	1·62	0·072	1·80	1·18

These values of M and p/p_{dry} have been added to figure 8.

REFERENCES

ALLEN, H. J. & PERKINS, E. W. 1951 *Nat. Adv. Comm. Aero., Wash., Rep.* no. 1048.

BURGESS, W. C. & SEASHORE, F. L. 1951 *Nat. Adv. Comm. Aero., Wash., Tech. Note,* no. 2158.

CRANE, J. F. W. 1959 *Roy. Aircraft Est., Rep.* no. Aero. 2616.

GAPCYNSKI, J. P. 1955 *Nat. Adv. Comm. Aero., Wash., Res. Mem.* no. L55H29.

GLAUERT, M. 1940 *Aero. Res. Coun., Lond., R. & M.* no. 2025.

HALL, I. M., ROGERS, E. W. E. & DAVIES, B. M. 1957 *Aero. Res. Coun., Lond., Tech. Note,* no. 19479 (F.M. 2574).

JORGENSEN, L. H. 1957 *Nat. Adv. Comm. Aero., Wash., Tech. Note,* no. 4045.

MASON, B. J. 1957 *The Physics of Clouds* (chap. IV, §4.3). Oxford: Clarendon Press.

MONAGHAN, R. J. 1956 *Aero. Res. Coun., Lond., Current Paper,* no. 247.

OSWATITSCH, K. 1941 *Aero. Res. Coun., Lond., Tech. Note,* no. 11348.

SANDER, A. & DAMKÖHLER, G. 1953 *Nat. Adv. Comm. Aero., Wash., Tech. Mem.* no. 1368.

SMOLDEREN, J. J. 1956 *AGARDograph,* no. 17.

STANBROOK, A. 1959 *Aero. Res. Coun., Lond., R. & M.* no. 3114.

STODOLA, A. 1927 *Steam and Gas Turbines* (Vol. I, p. 123), 6th ed. New York: McGraw-Hill.